γ

BNL-NCS-27050

CONF-791223--4

STATUS OF RADIATIVE WIDTHS, NEUTRON STRENGTH FUNCTIONS AND IMPROVED EVALUATION USING THE LANE-LYNN THEORY*

S. Mughabghab
National Nuclear Data Center
Brookhaven National Laboratory
Upton, N.Y. 11973

MASTER

ABSTRACT

The s- and p-wave neutron strength functions and average radiative widths of fission product nuclides are reviewed.

The direct capture mechanism of Lane and Lynn is quantitatively verified for the two reactions $^{42}Ca(n,\gamma)\,^{43}Ca$ and $^{136}Xe(n,\gamma)\,^{137}Xe$. Thermal capture cross sections of ^{132}Te and ^{126}Sn, are estimated with the aid of the Lane-Lynn theory.

Introduction

The investigation of the average parameters of neutron resonances (S_0, S_1, $\Gamma_{\gamma 0}$, $\Gamma_{\gamma 1}$, D_0, D_1, R') is of primary importance because these quantities play a major role in:

1) the optical model

2) reactor cycle and burn-up calculations

3) understanding the neutron reaction mechanisms of thermal and resonance neutrons.

For the prediction of the efficient and safe performance of thermal and fast reactors, it is necessary to have a knowledge of the capture cross sections in the thermal and fast regions of the various fission product (FP) nuclides produced in a reactor cycle. In some cases, either these FP isotopes are radioactive and/or experimental information is not available. Because of these difficulties, one has to resort to calculations of the capture cross section with the aid of average resonance parameters derived from theory (such as the optical model) and/or systematics of neighboring nuclides. Such a procedure is applied in the unresolved energy region. In the thermal

* Research supported by the U.S. Department of Energy.

region, in some favorable cases, one can predict the thermal capture cross section with the aid of the Lane and Lynn theory /1,2/.

Within the past five years, a great deal of experimental data on the individual resonance parameters has become available. In addition, numerous average capture and total cross section data from which average resonance parameters can be extracted have been carried out. This situation warranted a reexamination of the neutron resonance parameters and their average properties. The results of this study will be published in a fourth edition of BNL-325, Vol. 1.

The average neturon resonance parameters which I wish to cover here are the s- and p-wave neutron strength functions and average total radiative widths. The average level spacings are discussed by other speakers at this conference. In the last section, I would like to disucss the applicability of the Lane-Lynn theory /1/ in the calculations of thermal capture cross sections for two radioactive fission product nuclides, ^{132}Te and ^{126}Sn.

S- and P-Wave Neutron Strength Functions

The s- and p-wave neutron strength functions are defined by the relations:

$$S_0 = \frac{(g\Gamma_n^0)}{(D_0)} = \frac{\sum_j g\Gamma_{nj}^0}{\Delta E}, \tag{1}$$

$$S_1 = \frac{(g\Gamma_n^1)}{3(D_1)} = \frac{\sum_j g\Gamma_{nj}^1}{3\Delta E} \tag{2}$$

where the summation is carried out over N resonances in an energy interval ΔE. Two methods have been exploited in the determination of the strength functions S_0 and S_1:

1) In the region where resonances are well resolved and thus individual resonance parameters are available, S_0 and S_1 are determined by Eqs. 1 and 2, respectively.

2) In the unresolved region, the behavior of the average cross section, yields values of the strength functions.

It can be shown that on the assumption that only s- and p-wave resonance contributions are significant, the average total cross section in the keV energy range can be written in the form

$$\langle\sigma_T\rangle = 4\pi(R')^2 + 2\pi^2\lambda^2 \sqrt{E}\,(S_o + 3k^2R^2S_1) + 0\,(S_0)^2 \tag{3}$$

Usually, the contribution of higher order terms $0(S_0)^2$ in the keV energy region is small and can be neglected. The accuracy in determining the strength functions by this method depends largely on the accuracy of the average cross section and on our knowledge of R' in the keV energy region. In addition, Gibbons et al. /3/ applied the theory of Lane and Lynn /4/ to derive s- and p-wave strength functions from their extensive average capture measurements through the relation

$$\langle\sigma_{J\ell}\rangle = \frac{2\pi^2}{k^2} \langle\Gamma_\gamma\rangle S_\ell P_\ell \sqrt{E} \frac{g_J \varepsilon_{IJ}^{\ell} F(\alpha_{\ell J})}{\langle\Gamma_J\rangle} \tag{4}$$

All the symbols have their usual meaning and are defined in Ref. /3/. It is important to recall here that certain assumptions were made in the derivation of Eq. 4.

1) The strength functions S_ℓ, are independent of J and are $\ll 1$.

2) $D_J = Dobs/g_J$

3) Γ_γ is independent of J, ℓ, and energy.

4) $\Gamma = \Gamma_n + \Gamma_\gamma$. This indicates that inelastic channel is considered closed.

As is very well known at the present time, the first condition is satisfied. On the other hand, the third condition may not be fulfilled particularly in the 3s and 3p giant resonances where differences exist between s- and p-radiative widths. The nature of these differences arise because of nonstatistical effects, such as valence neutron capture and doorway state formation, and mode of decay of γ-rays to low lying states. Consequently, such differences in the radiative widths must be taken into account in applying Eq. 4.

The results which will be presented here are based largely on the evaluation of the experimental data which are compiled at the National Nuclear Data Center at Brookhaven National Laboratory and stored on magnetic tapes of the CSISRS library. At the present time, a major effort is devoted in the examination of the individual resonance parameter data for the purpose of coming up with recommended values which will be published in the report BNL-325, Vol. 1, 4th Edition. Before presenting the results, I would like to describe briefly our techniques. The various experimental data of measurers are transformed into a standard form (such as $g\Gamma_n$ values), are grouped according to resonance energy, and then a weighted average of the same quantities is computed. In addition internal and external errors are calculated. The evaluator then examines the results and makes any changes he may deem necessary. With the aid of another computer code, the recommended values are transformed into an ENDF format. Resonances with unknown spins and/or radiative widths are assigned spins and/or average Γ_γ with the provision that the (2J+1) law for the level density is satisfied. Subsequently, these recommended parameters are automatically fed into another program (BNLPSY) which performs calculations of the following quantities:

a) thermal capture and fission cross sections for each resonance

b) capture and fission resonance integrals for each resonance

c) coherent scattering amplitudes (the real and the imaginary parts) for each spin state

d) incoherent scattering cross sections for targets with $I \neq 0$

e) s- and p-wave strength functions

f) average radiative widths for s- and p-wave resonances.

Consequently, the evaluator examines the results and may make additional adjustments in the first few resonances or add bound levels in order to achieve agreement with the thermal cross sections and resonance integrals. Finally, a staircase plot is produced for s- and p-wave strength functions and level spacings. This is illustrated in Figs. 1-4 for ^{70}Zn.

The preliminary evaluated strength functions, S_0 and S_1 in units of 10^{-4} are presented in Columns 3 and 4 of Table I. For the most part, these are based on the individual resonance parameters. In some cases, because of a lack of $g\Gamma_n$ values, the recommended values are based on average cross section data. These are designated by an asterisk. In Column 2, the status of the strength function values is described by the letters a,b,c,d; the significance of which is as follows:

(a) = resonance parameter data is available after 1973

(b) = new measurements of resonance parameters have not been carried out after 1973

(c) = recent measurements carried out but the results of the analysis have not yet been published

(d) = parameters for 7 resonances of ^{134}Cs are available. However the result of the calculation of strength function for this isotope may not be satistically meaningful.

An examination of the status column indicates that improvements in our knowledge of the strength functions of the isotopes in the mass region A = 87-110 have been achieved. This is largely due to measurements carried out at ORELA and GEEL. Note that the average resonance parameters of the rare earth isotopes are not included here because their evaluation have not been completed.

At this point it is noteworthy to mention that Murty et al. /5/ reported capture measurements of nuclei in the mass region 63-140 using the activation technique and an Sb-Be photoneutron source ($E_n \approx 25$ keV). From these measurements these authors derived p-wave strength functions. On the basis of these determinations, they a ved at the conclusion that there is a splitting of the 3p size resonance with a minimum at A = 100 with $S_1 = 1.5 \times 10^{-4}$. This would require that the spin-orbit force is twice the normal value. This conclusion is at variance with the present results and with our present knowledge of the spin-orbit potential.

S- and P-Wave Total Radiative Widths

As pointed out previously, of particular importance in the calculations of capture cross section is an accurate determination of the radiative width of individual resonances in order to study its variation with mass number, excitation energy, spin and parity of the resonances. As is very well established now /6-8/, nonstatistical effects play an important role in the capture reaction mechanism particularly in the 3p size resonance, i.e., in the mass region 90-100. Because of this, the partial radiative decay amplitude (from an initial, j, state to a final state, f) can be written as a sum of several contributions

$$\Gamma^{\frac{1}{2}}_{\gamma jf} = \Gamma^{\frac{1}{2}}_{\gamma jf}\,(cn) + \Gamma^{\frac{1}{2}}_{\gamma jf}\,(ds) + \Gamma^{\frac{1}{2}}_{\gamma jf}\,(sp) \tag{5}$$

where the successive terms on the right-hand side correspond respectively to compound-nucleus, doorway state, and single particle effects. Therefore, the total radiative width of resonance j can be written as

$$\Gamma^{\frac{1}{2}}_{\gamma j} = \sum_{f} \Gamma^{\frac{1}{2}}_{\gamma jf} \tag{6}$$

If one assumes that the sign of the interference terms between direct capture and the statistical components is random, then:

$$\Gamma_{\gamma j} = \Gamma_{\gamma j}(cn) + \Gamma_{\gamma j}(ds) + \Gamma_{\gamma j}(sp) \tag{7}$$

It has been demonstrated in Ref. /6,7/ that the valence components in ^{90}Zr and ^{98}Mo can be as large as the statistical component particularly for resonances with large reduced neutron widths. Therefore, nonstatistical effects should be taken into consideration in the evaluation of capture cross sections in this mass region as well as in the 3s giant resonance region. For isotopes with A > 150, nonstatistical effects are negligible and can be ignored in the calculations of capture cross sections. Gruppelaar /9/ applied the valence neutron model in the evaluation of the capture cross sections of ^{90}Zr and ^{98}Mo.

Other methods which are based on the Brink-Axel representation and thermodynamics considerations have been applied with some success. Dr. Benzi will present at this meeting some results of total radiative widths based on the thermodynamical model. Moore /10/ presented at the Harwell conference calculations of total radiative widths for transactinium isotopes based on the Brink-Axel theory. Some success was achieved in these calculations. Finally, we note the recent theoretical calculations by Zaretskii and Sirotkin /11/ of the total radiative widths, which are carried out, in the framework of the shell approach using the theory of Fermi systems. A simple estimate is derived for the total radiative width which is given by:

$$\Gamma_\gamma = 3.1 \times 10^{-2} \left(\frac{U}{a} A^{2/3}\right)^{7/2} \tag{7}$$

where U and a^{-1} are the excitation energy and level density, respectively, expressed in MeV units. The radiative width Γ_γ is expressed in meV. (It is believed by the present reviewer that there is a typographical error in Eq. 26 of Ref. /11/.)

Next, let us turn our attention to the experimental values of the radiative widths of FP nuclides. The evaluated numbers are listed in Columns 5 and 6. Two features are readily evident from an examination of the numbers:

1) In the mass region spanning mass numbers 88 to 100, there are differences between the s- and p-wave radiative widths. Specifically, the p-wave radiative widths are larger than the s-wave radiative widths.

2) There is a general trend of a decrease of Γ_γ with mass number for both s- and p-wave resonances.

This dependence of Γ_γ on A has been known for some time. Recently, Malecky et al. /12/ analyzed the experimental data and deduced the following relation:

$$\Gamma_\gamma = 8.7\ U^{0.9-0.9}\ A^{-0.9} a^{-0.57} \tag{8}$$

As an approximateion, a α A, therefore, $\Gamma_\gamma \ \alpha \ A^{-1.47}$. This dependence of Γ_γ on mass number is in satisfactcory agreement with Zaretskii and Sirotkin's theory /11/.

The Potential Capture of Lane and Lynn

In the past few years a large body of thermal capture data in the mass regions around A=40 and 140 which exhibit positive correlation between "reduced" gamma ray intensities and (d,p) spectroscopic strengths has accumulated /13/. This indicates that the Lane and Lynn /1/ theory of channel capture plays a major role in the interactions of thermal neutrons with nuclear matter in these mass regions. At this point let us review briefly the expression for direct capture and discuss its validity and limitations. The capture of an s-wave neutron with energy E_n by a target nucleus of spin I to a final p orbit of spin J_f and spectroscopic factor S_{dp} is described by

$$\sigma_{\gamma f} = \frac{0.062}{RE_n^{1/2}} \left(\frac{Z}{A}\right)^2 \mu \frac{(2J_f + 1)}{6(2I + 1)} S_{dp} y_f^2$$

$$\times \left[\frac{(y_f + 3) + (y_f - y_{fs})(y_f + 2)}{(y_f + 1)}\right]^2 , \tag{9}$$

where

$$y_f^2 = R^2 k_f^2 = R^2 2mE_\gamma/h^2,$$

$$y_{fs}^2 = a_{coh}^2 \, 2mE_\gamma/h^2.$$

The interaction radius R is set equal to 1.35 $A^{1/3}$. It is assumed that for an odd target nucleus, there are equal contributions from channel spins I + 1/2 and I - 1/2. The variable μ takes into account the multiplicity due to the incident-neutron channel spin. For I=0, μ=1; however, for a target nucleus with nonzero spin, I,

$$\mu = 1 \quad \text{for } J_f = I \pm 3/2,$$
$$\mu = 2 \quad \text{for } J_f = I \pm 1/2.$$

It is emphasized that the resonance contribution, due to compound nucleus formation is assumed to be negligible, i.e., positive and/or negative neutron energy resonances, are not located close to thermal energy. Note that for the cases where $\Gamma_{n,j}/E_j \ll 1$, $a_{coh} = R'$. As a result, the partial direct capture cross section can be written as

$$\sigma_{\gamma f} = \frac{0.062}{R \;\; E_n} \left(\frac{Z}{A}\right)^2 \mu \frac{2J_f+1}{6(2I_t+1)} S_{dp} \left(\frac{y_f+3}{y_f+1}\right)^2 y_f^2$$

$$\times \left[I + \frac{R-R'}{R} \; y_f \frac{y_f+2}{y_f+3}\right]^2 \tag{10}$$

The total direct capture corss section is a summation of terms carried out over final states, f.

$$\sigma_\gamma \text{ (direct)} = \sum_f \sigma_{\gamma f}$$

It is interesting to note the following features;

1) There is a strong variation of the direct capture cross section with mass number through the term (R-R')/R. This can be shown by examination of Fig. 5 where the scattering radius R' is plotted versus mass number. Note that two minima occur at mass numbers 40 and 142. The minimum at 142 is important for our purposes here since it represents a maximum in the fission product yield.

2) Since the direct capture cross section is directly proportional to the (d,p) spectroscopic strength, it will be enhanced for those nuclei near magic numbers, for example at mass numbers near A = 138.

At this stage, let us turn our attention to the verification of the theory by presenting two examples; ^{42}Ca and ^{136}Xe for which γ-ray spectra measurements have been carried out.

The results of the calculations for ^{42}Ca via expression /10/ are summarized in Fig. 6. On the right-hand side are shown the calculations for each transition, while on the left-hand side are presented the experimental partial capture cross sections obtained with the aid of the relation $\sigma_\gamma = I_{\gamma f}\sigma_\gamma$. As indicated, there is very good agreement between the experimental and calculated values for each partial capture cross section and consequently for the summation of the partial capture cross sections.

The comparison between theory and experiment for the reaction ^{136}Xe (n,γ) ^{137}Xe is illustrated in Fig.7. Again very good agreement is observed between calculations and measurements.

In WRENDA 76/77, two requests (No. 428, 420) for the thermal capture cross sections ^{132}Te(n,γ) ^{133}Te and ^{126}Sn(n,γ) ^{127}Sn are noted for the object of calculations of fission product poisons. Both of these nuclides are radioactive with half lives of 78h and 12.4d, respectively. Because of the well known experimental difficulties of obtaining samples for these isotopes, such data is not readily available as yet. Since both of these nuclides are even-even and they are situated in the vicinity of the mass region where the p-wave strength function peaks, it is expected that s-wave resonances are not situated close to thermal energy. Because of these considerations, one can carry out the calculations in the framework of the Lane-Lynn theory on the assumption that the single particle (d,p) spectroscopic strengths in ^{132}Te and ^{126}Sn are the same as in ^{130}Te and ^{124}Sn for which experimental data are available. The results of the calculations are:

$$^{132}Te(n,\gamma)\,^{133}Te \qquad \sigma_\gamma = 0.135 \text{ b},$$
$$^{126}Sn(n,\gamma)\,^{127}Te \qquad \sigma_\gamma = 0.120 \text{ b}$$

We emphasize that if low-lying resonances are located near thermal energies, these values then would represent a lower limit for the capture cross section.

REFERENCES

1. A.M. Lane and J.E. Lynn, Nucl. Phys. 17, 563, 586 (1961).
2. S.F. Mughabghab, Phys. Lett. 81B, 93 (1979).
3. J.H. Gibbons, R.L. Macklin, P.D. Miller, and J.H. Neiler, Phys. Rev., 122, 182 (1961).
4. A.M. Lane and J.E. Lynn, Proc. Phys. Soc. (London) A70, 557 (1957).
5. M.S. Murty, K. Siddapa, J. Rama Rao, Nucl. Phys. A213, 35 (1973).
6. S.F. Mughabghab, R.E. Chrien, O.A. Wasson, G.W. Cole, and M.R. Bhat, Phys. Rev. Lett. 26, 1118 (1971).
7. R.E. Toohey and H.E. Jackson, Phys. Rev. C9,346 (1974).
8. S.F. Mughabghab, III International School on Neutron Physics, p.328, Alushta (1978).
9. H. Gruppelaar, Internal Report FSR-Gr-42, Petten (1976).
10. M.S. Moore, Neutron Physics and Nuclear Data, p. 313, Harwell, Sept. 1978.
11. D.F. Zaretskii and V.K. Sirotkin, Yad. Fiz, 27, 1534 (1978).
12. H. Malecky, L.B. Pikelner, I.M. Salamatin, and E.I. Sharapov, Yad. Fiz. 13, 240 (1971).
13. J. Kopecky and C. Plug, RCN-75-004 (1974).

Table I. Summary of the s- and p-Wave Strength Functions and Average Radiative Widths of Fission Product Nuclides in the Mass Region 85-147

Isotope	Status	S_0	S_1	$\Gamma_{\gamma 0}$(eV)	$\Gamma_{\gamma 1}$(eV)
Rb-85	b	1.0 ± 0.4		0.205	
Rb-87	b	1.6 ± 0.9			
Sr-86					
Sr-87	a	0.30 ± 0.07		0.310	
Sr-88	a	0.45 ± 0.23	5.0 ± 0.8	0.225	0.720
Y-89	a	0.27 ± 0.05	2.64 ± 0.03	0.130	0.300
Zr-90	a	0.7 ± 0.2	4.0 ± 0.6	0.240	0.440
Zr-91	a	0.36 ± 0.08	6.7 ± 1.3	0.140	0.240
Zr-92	a	0.5 ± 0.1	7.0 ± 1.3	0.140	0.360
Zr-94	a	0.50 ± 0.15	9.8 ± 2.0	0.130	0.185
Zr-96	a	0.34 ± 0.14	6.0 ± 1.8		
Nb-93	a	0.89 ± 0.10	4.7 ± 1.0	0.160	0.200
Mo-95	a	0.40 ± 0.06	4.0 ± 2.0	0.160	0.250
Mo-96	a	0.5 ± 0.2		0.110	
Mo-97	a	0.29 ± 0.02		0.140	0.180
Mo-98	a	0.5 ± 0.1	7.3 ± 1.1	0.085	0.125
Mo-100	a	0.7 ± 0.2	5.0 ± 1.1	0.088	0.098
Tc-99	a	0.45 ± 0.05			
Ru-99	b	0.72 ± 0.16			
Ru-100	a		6.5 ± 0.9*		
Ru-101	a	0.59 ± 0.04*	6.1 ± 0.4*		
Ru-104	a		5.0 ± 0.4*		
Ru-106	a		5.7 ± 0.9*		
Rh-103	a	1.04 ± 0.13*	7.9 ± 0.7*		
Pd-105	a	0.60 ± 0.10*	5.8 ± 0.6	0.145	
Pd-106	a	0.50 ± 0.05*	6.7 ± 0.6*		
Pd-108	a	0.78 ± 0.17*	5.9 ± 0.6*		
Pd-110	a	0.40 ± 0.06*	8.1 ± 0.9*		
Ag-107	b	0.38 ± 0.07	3.8 ± 0.6	0.140	
Ag-108	b	0.46 ± 0.15	3.8 ± 0.6	0.130	
Cd-111	b	0.45 ± 0.06			
Cd-112	b	0.58 ± 0.08			
Cd-113	b	0.32 ± 0.07			
Cd-114	b	0.54 ± 0.11			
Cd-116	b	0.21 ± 0.06			
In-115	b	0.26 ± 0.03	2.5 ± 0.5		
Sn-115	b				
Sn-117	b	0.19 ± 0.02	3.0 ± 1.6		
Sn-118	b	0.40 ± 0.15			
Sn-119	b	0.08 ± 0.03	3.8 ± 1.5		
Sn-120	a	0.14 ± 0.02	2.1 ± 0.2		
Sn-122	b				
Sn-124	b				
Sb-121	b	0.29 ± 0.05	1.1 ± 0.10		
Sb-123	b	0.22 ± 0.07	2.0 ± 1.5		
Te-125	b,c	0.49 ± 0.10			
Te-126	b,c	0.30 ± 0.10			
Te-128	b,c	0.25 ± 0.15			
Te-130	b,c	0.14 ± 0.05			

Table I. (cont.)

Isotope	Status	S_0	S_1	$\Gamma_{\gamma 0}$(eV)	$\Gamma_{\gamma 1}$(eV)
I-127	a	0.76 ± 0.06		0.090	
Xe-129	b,c	1.0 ± 0.2			
Xe-130	b,c	1.3 ± 0.5			
Xe-131	b,c	0.70 ± 0.16			
Xe-132	b,c				
Xe-134	b,c				
Xe-136	b,c				
Cs-133	a	0.70 ± 0.08		0.120	
Cs-134	d				
Ba-135	a	0.39 ± 0.07		0.141	
Ba-136	a	1.2 ± 0.5		0.126	
Ba-137	a	1.4 ± 0.4		0.084	
Ba-138	a	2.0 ± 0.5		0.108	
La-139	b	0.75 ± 0.11		0.060	
Ce-140	b	1.1 ± 0.2	0.34 ± 0.05		
Ce-142	a				
Pr-141	b	1.5 ± 0.2		0.086	
Nd-143	a	3.3 ± 0.4		0.081	
Nd-144	a	4.4 ± 1.0		0.055	
Nd-145	a	4.0 ± 0.4		0.075	
Nd-146	a	2.3 ± 0.5		0.054	
Nd-148	a	3.1 ± 0.5	0.3 ± 0.1	0.051	
Nd-150	a	2.9 ± 0.3		0.067	

(a) Resonance parameter data available after 1973.
(b) Measurements have not been carried out after 1973.
(c) Recent measurements carried out but results are unavailable.
(d) Recent results of 7 resonances available for this radioactive isotope.

* Results derived from average cross section data.

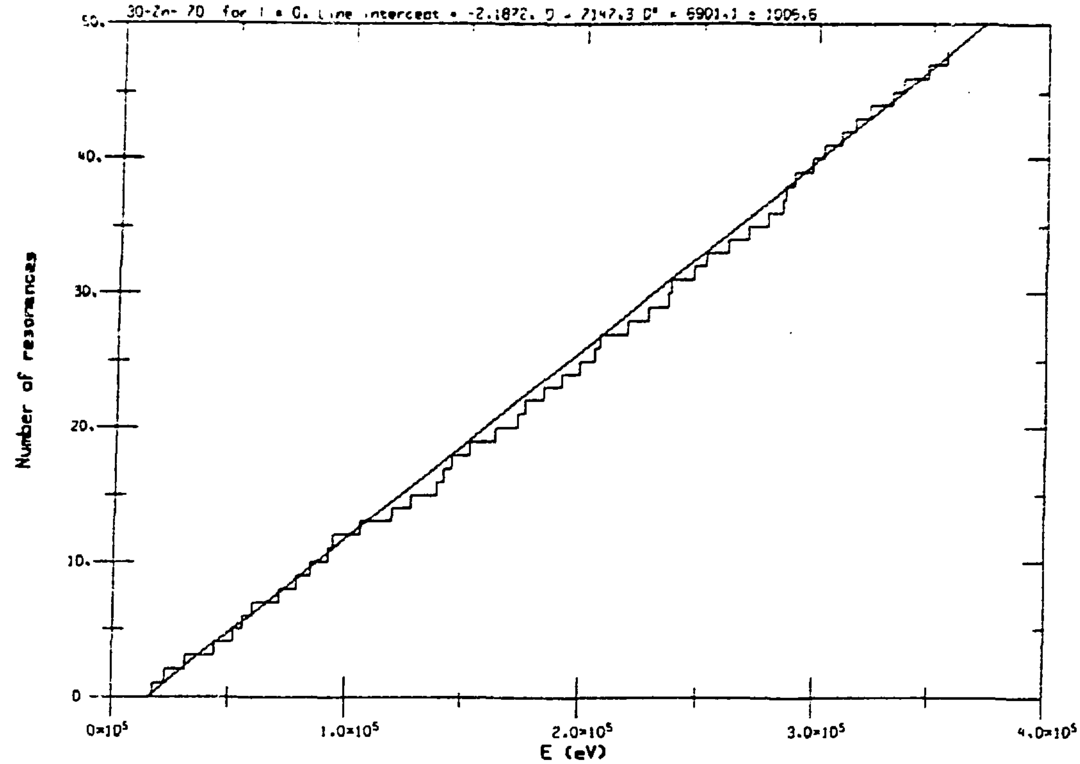

Fig. 1 Cumulative number of s-wave resonances of ^{70}Zn as a function of neutron energy. The data are based on measurements by Garg et al. (private communication).

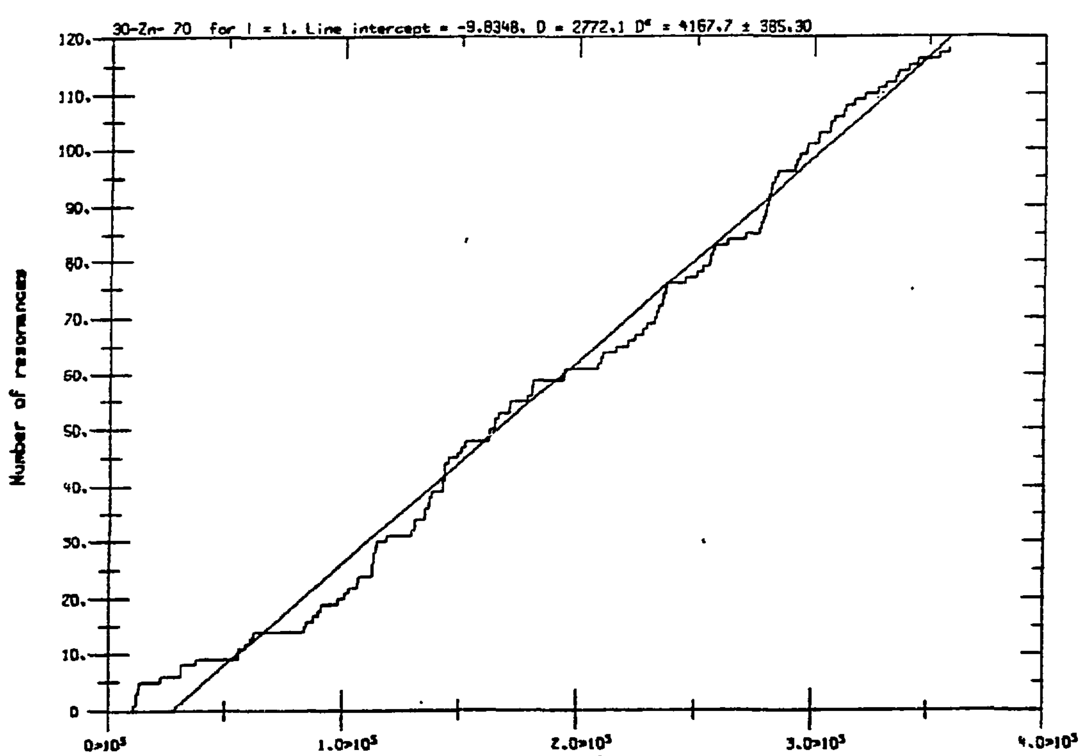

Fig. 2 Cumulative number of p-wave resonances of ^{70}Zn as a function of neutron energy. The data are based on measurements by Garg et al. (private communication).

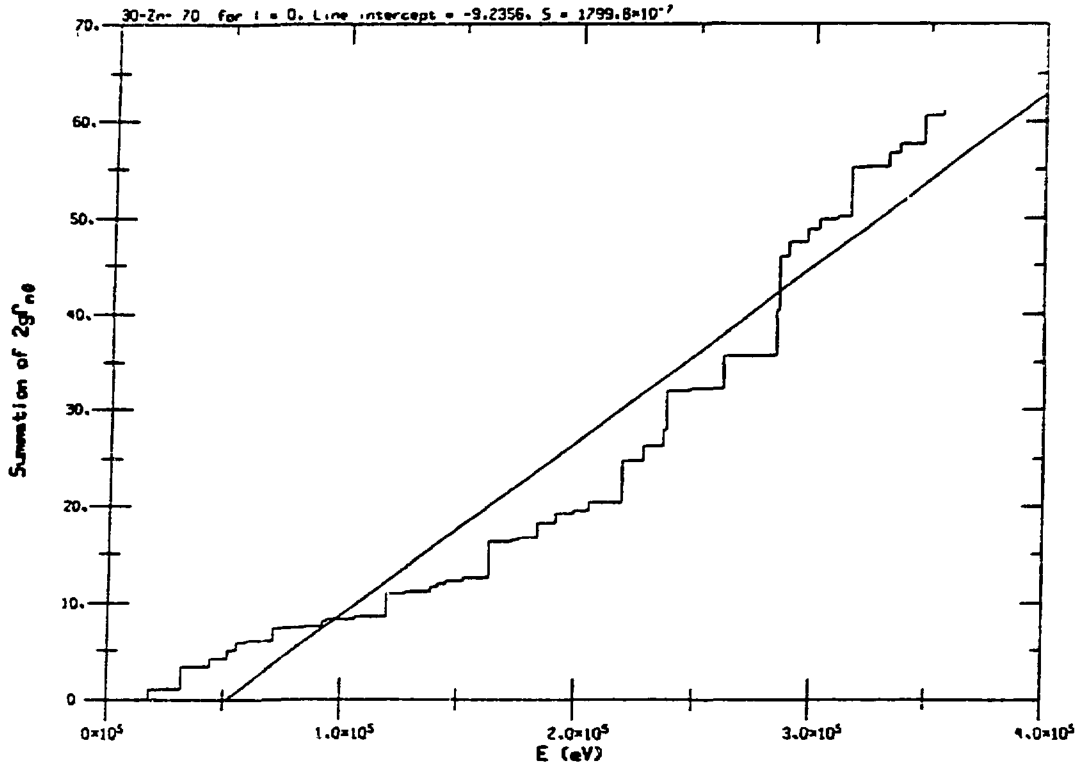

Fig. 3 Staircase plot of the s-wave reduced neutron widths of ^{70}Zn versus neutron energy. From such plots the s-wave neutron strength function is deduced.

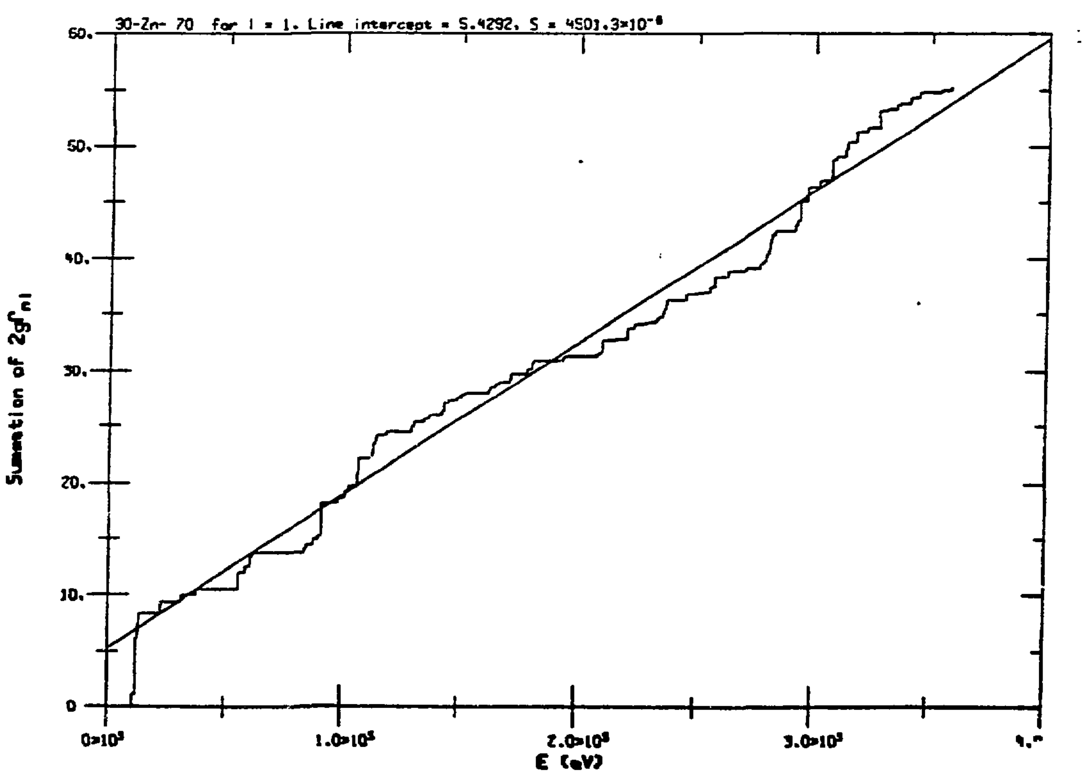

Fig. 4 Staircase plot of the p-wave reduced neutron widths of ^{70}Zn versus neutron energy.

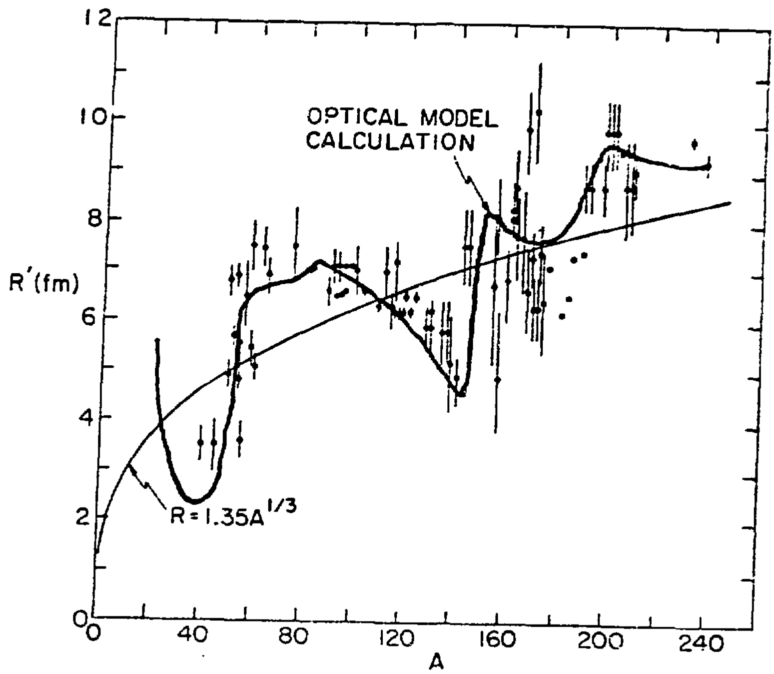

Fig. 5 Variation of the scattering radius as a function of mass number. Note the deep minima at mass numbers 40 and 140. The solid curve passing through the points is an optical model calculation.

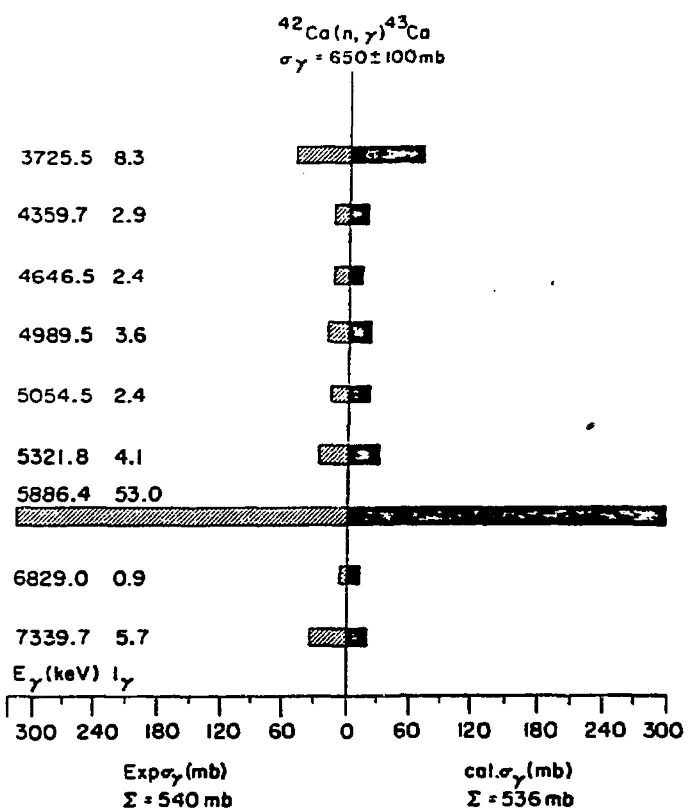

Fig. 6 Comparison of partial capture cross sections with the Lane-Lynn predictions for $^{42}Ca(n,\gamma)\ ^{43}Ca$.

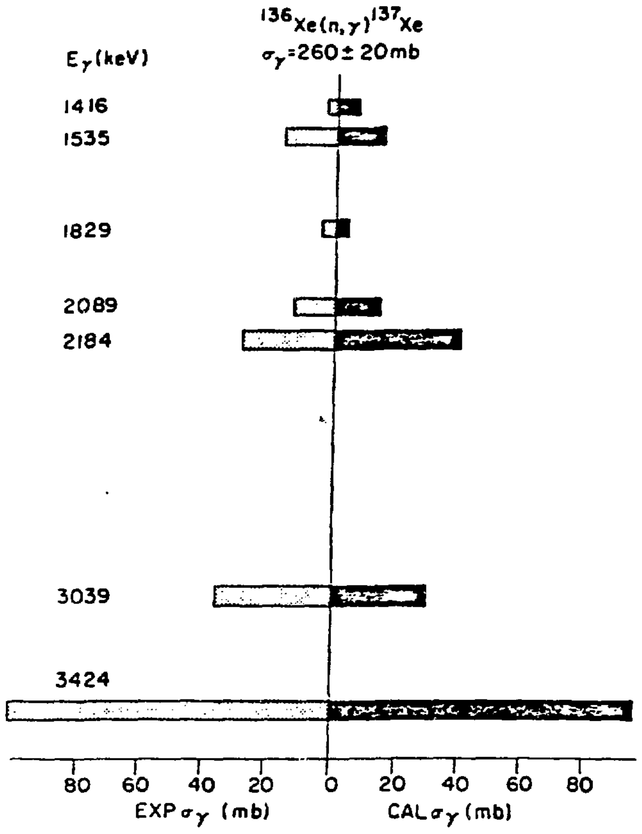

Fig. 7 Comparison of measured and calculated partial cross sections for ^{136}Xe (n,γ) ^{137}Xe.